water

Article

Analysis of Groundwater Storage Fluctuations Using GRACE and Remote Sensing Data in Wadi As-Sirhan, Northern Saudi Arabia

Fahad Alshehri [1,*] and Ahmed Mohamed [1,2]

[1] Abdullah Alrushaid Chair for Earth Science Remote Sensing Research, Geology and Geophysics Department, College of Science, King Saud University, Riyadh 11451, Saudi Arabia
[2] Geology Department, Faculty of Science, Assiut University, Assiut 71516, Egypt
* Correspondence: falshehria@ksu.edu.sa; Tel.: +966-11-4677053

Abstract: Human activity has led to a rise in the demand for water, prompting Saudi Arabia to search for alternative groundwater supplies. Wadi As-Sirhan is one area that has experienced extensive agricultural growth and the severe over-exploitation of its groundwater resources. The groundwater drawn from the wadi should be continuously monitored to determine the best management options for groundwater resources and economic growth. The most recent Gravity Recovery and Climate Experiment (GRACE) mission and outputs of land surface models were combined to estimate the depletion rate of the groundwater of the Wadi As-Sirhan drainage basin in the northern region of Saudi Arabia throughout the period of April 2002–December 2021. The findings are: (1) the average GRACE-derived terrestrial water storage variation (ΔTWS) was calculated at -13.82 ± 0.24 mm/yr; (2) the soil moisture storage variation was averaged at $+0.008 \pm 0.004$ mm/yr; (3) the GRACE-derived groundwater depletion rate was estimated at -13.81 ± 0.24 mm/yr; (4) the annual precipitation data over the Wadi As-Sirhan was averaged at 60 mm/yr; (5) The wadi has a minimal recharge rate of $+2.31 \pm 0.24$ mm/yr, which may partially compensate for a portion of the groundwater withdrawal; (6) the sediment thickness shows an increase from 0 m at the southern igneous and volcanic rocks to more than 3000 m close to the Saudi–Jordanian border; (7) The wadi's eastern, southern, and western portions are the sources of its tributaries, which ultimately drain into its northwestern portion; (8) change detection from the Landsat photos reveals considerable agricultural expansions over recent decades. The integrated method is useful for analyzing changes to groundwater resources in large groundwater reservoirs and developing environmentally appropriate management programs for these resources.

Keywords: gravity data; groundwater resources; depletion; Wadi As-Sirhan; Saudi Arabia

Citation: Alshehri, F.; Mohamed, A. Analysis of Groundwater Storage Fluctuations Using GRACE and Remote Sensing Data in Wadi As-Sirhan, Northern Saudi Arabia. *Water* **2023**, *15*, 282. https://doi.org/10.3390/w15020282

Academic Editor: Alexander Yakirevich

Received: 6 December 2022
Revised: 1 January 2023
Accepted: 4 January 2023
Published: 9 January 2023

1. Introduction

The Wadi As-Sirhan drainage basin is located in the northwest of Saudi Arabia, about 1000 km north of Jeddah. It is located between 26.25° and 31.77° N latitude, and 37° and 41° E longitude (Figure 1). It includes Saudi Arabia's western border with the Hashemite Kingdom of Jordan.

Some of the world's largest sand and gravel deserts may be found in northern Saudi Arabia [1], but due to advances in agricultural technology, their appearance has altered [1]. Even as recently as 1986, the Wadi As-Sirhan area saw almost no cultivation. However, the Saudi government has been consistently investing oil sector income in agricultural fields for the previous 26 years. Wheat, fruits, and vegetables are among the crops that thrive in this region [1].

For the purpose of crop irrigation in the fields, water is pumped up from a subterranean aquifer. The Al-Disi aquifer is mostly buried beneath the Saudi Arabian desert, although a small portion of it can be found in the northwest corner of Jordan.

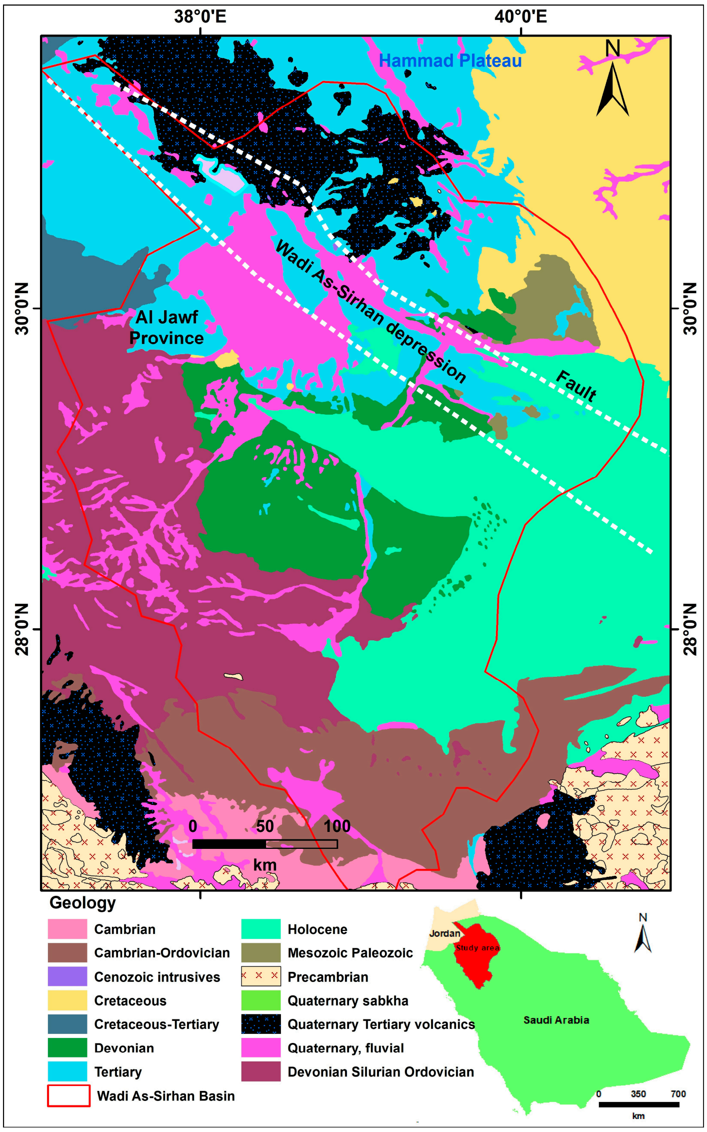

Figure 1. Showing the study area's geology.

Groundwater aquifers are tapped to supply irrigation systems for the farms. Center-pivot agriculture rotates the water source around a central point in a circular field [1]. Better water and fertilizer management are only two of the advantages this method offers over conventional surface irrigation. This type of "precise agriculture" is crucial in places where evaporation wastes a lot of water. A reduction in evaporative losses can be achieved through more precise water management applications [1].

People have been taking groundwater out of the Wadi As-Sirhan region since 1986, changing it, and the groundwater storage is always going down [2]. Because geophysical methods have recently become more advanced, it is now possible to monitor groundwater depletion over a large area.

The Gravity Recovery and Climate Experiment (GRACE) satellite mission can detect fluctuations in mass caused by changes in the amount of terrestrial water storage (ΔTWS) stored on land. To study the dynamic changes in Earth's mass over space and time, the mission was started in March 2002 by NASA and the German Aerospace Center (GFZ) to detect and quantify changes in the Earth's gravity. The GRACE-extracted terrestrial water storage (ΔTWS) consists of several components, such as soil moisture and groundwater.

NASA and GFZ launched the GRACE Follow-On (GRACE-FO) mission as a continuation of the GRACE mission [3]. This mission came after the first GRACE project, which went around the Earth from 2002 to 2017. It builds on what its predecessor did well and tests new technology that makes measurements much more accurate.

It also provides data to the monthly global high-resolution models of the Earth's gravitational field that were initiated during the GRACE mission. The GRACE and GRACE-FO Science Data System receives monthly gravity solutions from the Jet Propulsion Laboratory (JPL), the NASA Goddard Space Flight Center (GSFC), and the University of Texas at Austin, Center for Space Research (CSR). GRACE data has been extensively utilized for analyzing aquifer storage variations and monitoring the time-varying mass distribution on Earth, as well as addressing previously unresolvable hydrogeological and climatological questions (e.g., [4–56]).

Ref. [57] figured out how fast the water in the Saq aquifer is being used up and what is causing this. In addition to depletion rates, [42] calculated the rate at which the Saq aquifer is being recharged. Ref. [39] have conducted integrated geophysical and remote sensing studies to examine land deformational features over the Lower Mega Aquifer System in northern and central Saudi Arabia and estimated the groundwater depletion rates during the period of April 2002–March 2016.

Sound management options for groundwater resources and the economic development of arid and semiarid areas such as the Wadi As-Sirhan region require an understanding of the hydrogeologic settings of groundwater aquifers as well as the recharge and discharge rates of these systems [58]. Aquifer systems' recharge, discharge, and depletion rates have been evaluated using a wide range of physical, chemical, and mathematical approaches [59–62]. The limited availability of datasets necessary for the execution of these methodologies, as well as the substantial time and resources needed to acquire them, make their results sometimes questionable and make it difficult to apply them on regional levels. Therefore, we have used GRACE data with the results of the Global Land Data Assimilation System (GLDAS) model to estimate changes in the Wadi As-Sirhan Basin's groundwater storage (ΔGWS) and the controlling factors. Wadi As-Sirhan must address the excessive exploitation of groundwater and the lowering groundwater table. These challenges require more attention.

The remainder of the article is structured as shown below. Important characteristics of the study region are shown in Section 2. The data type and sources and the methodology suggested in the study are provided in Section 3. The findings and discussions of the study's many analyses are presented in Section 4. Finally, Section 5 offers the concluding observations.

2. Geology and Hydrogeology

The Wadi As-Sirhan region is located in the west-central region of the Sirhan-Turayf basin in the northwestern region of the kingdom, close to the border with Jordan (Figure 1). It is composed of Devonian sandstone, lower tertiary sedimentary rocks of the Turayf group, Tertiary and Quaternary basalt, and unconsolidated sedimentary deposits [63]. The major structural element of the region is the Wadi As-Sirhan graben (WASG). The Sirhan-Turayf Basin is a shallow area of sediments that goes west and north into Iraq and Jordan. The sedimentary rocks and surface sediments range in age from Cambrian to recent and are approximately 2300 m thick [64]. The Hail Arch, a large anticlinal feature on the basin's eastern edge, may serve as a dividing line between the sedimentary facies of the Arabian Gulf and the Mediterranean Basin [64]. The WASG complex is bordered to the west by the Al Busayta fault and to the east by the Al Khalad–Al Misma faults and Wadi As-Sirhan. Clearly evident in both satellite and aerial images are lineaments that go northwest to northeast. Those on the western edge are likely associated with the WASG's movement, whereas those on the eastern edge may be associated with uplift and other structural movements along the Hail Arch. The vast lava field in the center of the Sirhan-Turayf Basin, the majority of which is seen on the map, was formed during the Tertiary and Quaternary epochs of volcanism. The main part of the study area is a structural depression formed by the WASG complex. It is surrounded by moderate highlands. The WASG is thought to have been created by forces of tension caused by the Red Sea tearing apart. Phosphorite, limestone uranium, opaline clay stone, lignite, oil, and gas are all possible resources in the Wadi As-Sirhan region [63]. The Mega Aquifer System (MAS) spans the Arabian Shelf across the countries of Saudi Arabia, the United Arab Emirates, Yemen, Qatar, Jordan, Oman, and Kuwait and represents the region's most important aquifers. Paleozoic sandstone sediments, marine Mesozoic carbonates, Cenozoic carbonate formations of Paleogene age, and Neogene sediments and volcanics constitute the primary aquifers of the MAS [65]. The MAS is essentially represented by two groups, with the Hith anhydrite sediments acting as a boundary between the two: the Lower Mega Aquifer System that consists of the Saq, Tabuk, Wajid, Minjur, Tawil, and Dhruma formations, and the Upper Mega Aquifer System (UMAS), which disappears in northern and northwestern regions of Arabia, that consists of the Biyadh, Aruma, Wasia, Rus, Umm Er Radhuma, and Dammam formations. The LMAS in the Wadi As-Sirhan region consists of the Saq (the major aquifer, but it is deep and undeveloped) and the overlying Tawil, Tabuk, Jubah, and Jauf, and the Secondary–Tertiary–Quaternary complex (SQT) as aquifers of local productivity [39,66].

3. Data and Methods

Most of the GRACE information used in this research comes from the mascon (mass concentration) solutions, which have higher spatial resolution and less inaccuracy than the raw GRACE data alone while still capturing all of the signals that GRACE detected. When working with the mascon solutions, spectral de-striping and smoothing filtering are unnecessary. In addition, no scaling technique is necessary [3,67–69].

The monthly gravity field fluctuations are provided by JPL mascon data, RL06, v. 1, with a $0.5^\circ \times 0.5^\circ$ grid. A portion of these mass change signals that span coasts also comprise signals from the ocean and the land. The entire mascon solution underwent post-processing with the Coastal Resolution Improvement filter to identify land and ocean masses from mascons that traverse coastlines [3]. When compared to the RL05 version, the grid used by the CSR mascon products in Release 06, v. 01 and a $0.25^\circ \times 0.25^\circ$ grid [69,70] is different. We used GSFC, RL06 v1.0 mas-con data, which were calculated for each 0.5 equal-area square mascon, in addition to the JPL and CSR mascon datasets.

The temporal variations in GRACE-derived ΔTWS data are derived over the specified area using the three different GRACE solutions. We used the linear interpolation method to fill in the missing monthly data (gap-filled time series). A trend and a seasonal term were simultaneously fitted to each ΔTWS time series, which allowed us to extract the secular trend. This procedure then estimates the errors that come along with the derived trend values.

Lacking or having inadequate data from ground-based stations in the research area throughout the study period, estimates of soil moisture (ΔSMS) are derived from the GLDAS model [4]. The ΔTWS was broken down into its primary parts using these results based on the following equation. This is because the GRACE has not been updated to properly identify the various ΔTWS components. Land surface models such as GLDAS use data from around the world with information from satellites and the ground to create the most accurate possible simulations for climate studies [4,71]. The VIC, NOAH, and CLM versions of the NSAS GLDAS were used in this research. The same time frame as the GRACE data was covered by the monthly data, which have a spatial resolution of one degree.

$$\Delta \mathrm{TWS} = \Delta \mathrm{GWS} + \Delta \mathrm{SMS} \tag{1}$$

Due to the absence of precipitation records from ground stations, we constructed a monthly time series of rainfall and annual average precipitation (AAP) from Tropical Rainfall Measuring Mission (TRMM) satellite data. The AAP rate was determined by arithmetically averaging the monthly rainfall data for a year. In this study, we used it to learn more about how precipitation affected the ΔGWS over the course of the experiment's time frame. Figure 2 illustrates the methods of the study.

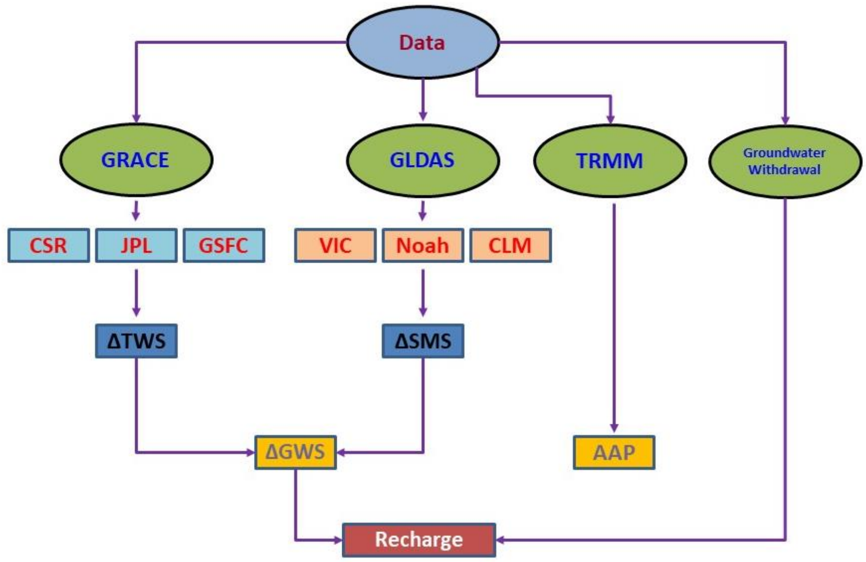

Figure 2. The methodological framework of the study.

4. Result and Discussion

In this work, we take a broad look at the groundwater possibilities of Wadi As-Sirhan in the northwestern region of Saudi Arabia by integrating GRACE and GLDAS satellite data.

4.1. Average Annual Precipitation

In Figure 3a, the monthly precipitation rate is plotted, with greater values between October and April and decreasing values between May and September. Higher values of approximately 116 mm can be observed in the northeastern part of the wadi from the AAP map (Figure 3b), whereas lower values can be seen up to 30 mm in the southwestern parts. According to Figure 3c, an annual rainfall time series, 2018 had the highest rate (105 mm), whereas 2004, 2007, 2011, 2012, 2016, and 2017 had the lowest rate (<40 mm). The AAP rate was estimated to be 60 mm for the study region throughout the period (2002–2019), reflecting that the study region is dry.

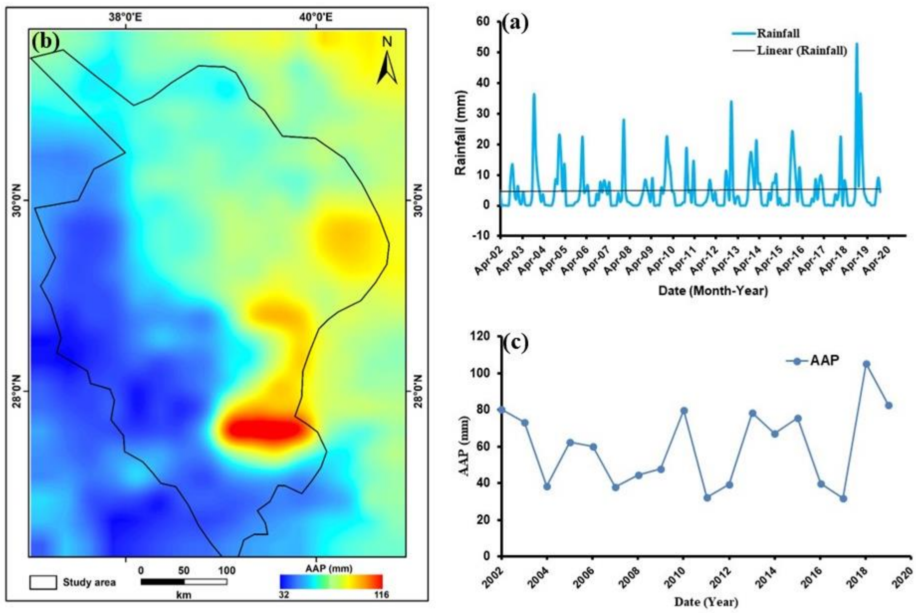

Figure 3. (**a**) Monthly average rainfall (mm), (**b**) the AAP (mm), and (**c**) the AAP times series calculated using TRMM data for the study region.

4.2. Temporal Variations in ΔTWS

Figure 4 illustrates the spatial distribution of the secular ΔTWS trends calculated from CSR and GFCF solutions from 2002 to 2021. Figure 4 indicates that the ΔTWS trend shows higher negative values varying between −20.5 and −22.9 mm/yr along the mainstream and the southeastern part of the wadi using CSR and GFCF datasets, respectively. The ΔTWS trend values are increasing towards the northeast and southwest directions reaching values varying between −5.5 and −4.5 mm/yr.

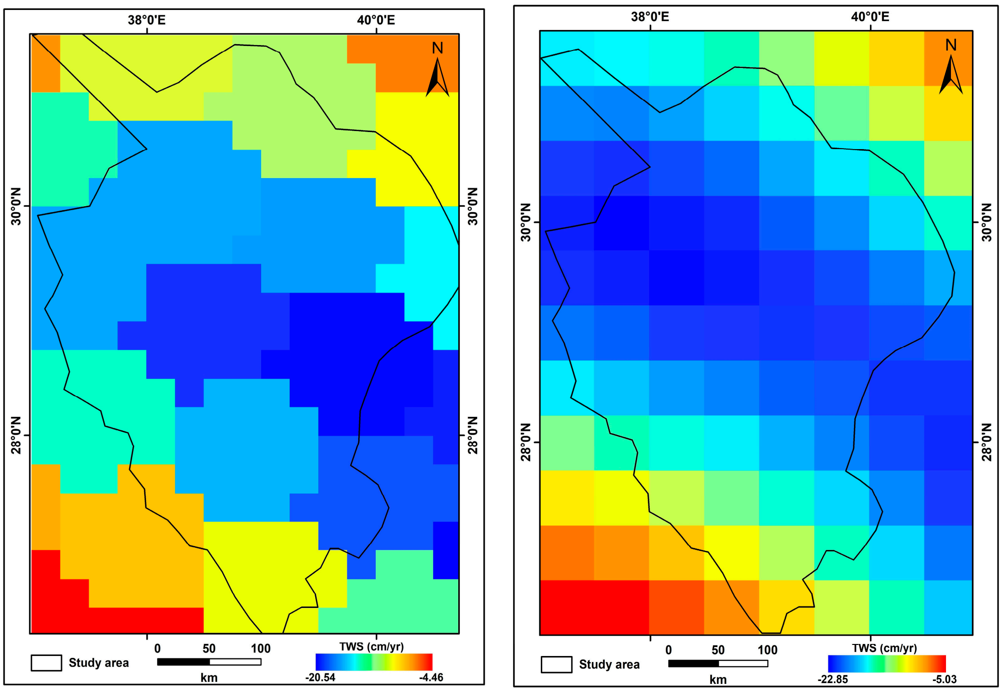

(**a**) (**b**)

Figure 4. Monthly TWS estimates from April 2002 to December 2021, produced from CSR (**a**) and GFCF (**b**) data, are displayed on a map with a color-coded secular TWS trend (mm/yr^{-1}).

Using GRACE estimates of ΔTWS for the research area, Figure 5 shows the monthly fluctuations in storage anomalies. Higher negative ΔTWS trend values, assessed at −12.32 ± 0.36, −13.3 ± 0.019, and −15.84 ± 0.31 mm/yr (Table 1) using CSR, JPL, and GFCF mascon solutions, respectively, for the study region over the studied period. The averaging of the three ΔTWS solutions for Wadi As-Sirhan during that period yielded a value of −13.82 ± 0.24 mm/yr (Table 1; Figure 5).

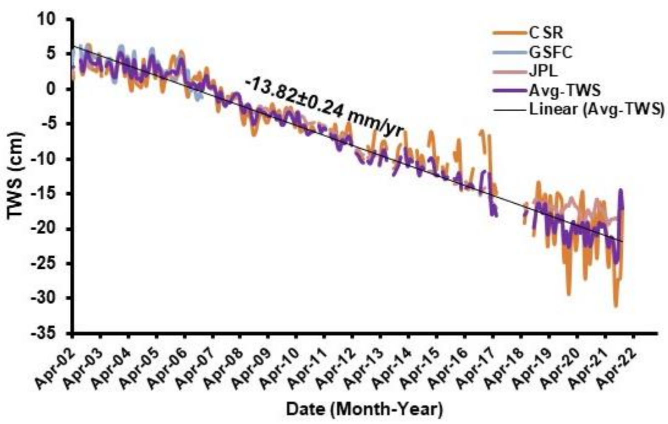

Figure 5. Monthly ΔTWS time series of the three mascon solutions and their averaging for the study area.

Table 1. ΔTWS parts (mm/yr^{-1}) for the entire study region with a confidence level of 95%.

Component (mm)		Entire Period
GRACE total (ΔTWS)	CSR	−12.32 ± 0.36
	JPL	−13.3 ± 0.019
	GSFC	−15.84 ± 0.31
	AVG	−13.82 ± 0.24
ΔSMS		+0.008 ± 0.004
ΔGWS		−13.81 ± 0.24
Groundwater withdrawal		−16.12 ± 0.0
Recharge		+2.31 ± 0.24
AAP		60.0

4.3. Temporal Variations in ΔSMS

Given the low precipitation rates over the study area, the GLDAS-derived ΔSMS exhibits a very minor upward trend throughout the investigated period. The estimated ΔSMS trend from the three GLDAS versions (VIC, CLM, Noah) for the study period is +0.008 ± 0.004 mm/yr (Table 1; Figure 6). Additionally, depicted in Figure 6 is the spatial distribution of the SMS trend across the research area.

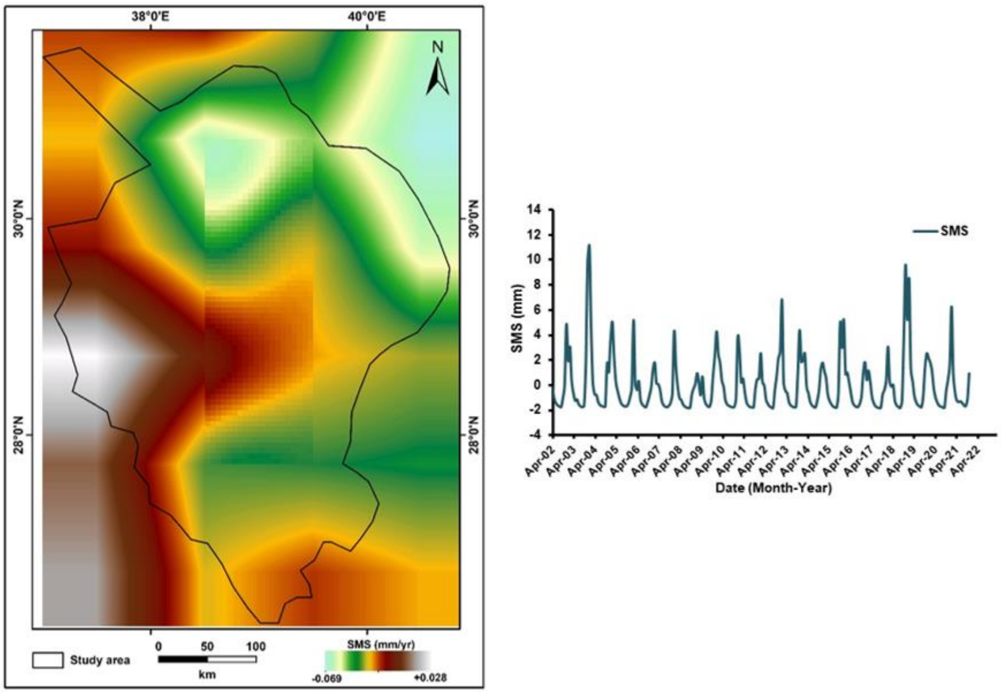

Figure 6. Spatiotemporal distribution and the monthly time series of the SMS trend for the entire study area.

4.4. Temporal Variations in ΔGWS

As was previously mentioned, GRACE is unable to tell the difference between abnormalities caused by various ΔTWS partitions (i.e., soil moisture, surface water, groundwater). Thus, the ΔTWS portions of the GLDAS model were used to estimate the non-groundwater components represented by ΔSMS changes.

By deducting the GLDAS-extracted ΔSMS storage from the GRACE-extracted ΔTWS, the ΔGWS was calculated using Equation (1). Similar to the ΔTWS, the ΔGWS (Figure 7) demonstrates greater values between October and April and lower values between May and September. CSR, JPL, and GFCF each provide estimates for the rate of change in GWS, with their averaging rate of −13.81 ± 0.24 mm/yr (Table 1; Figure 7).

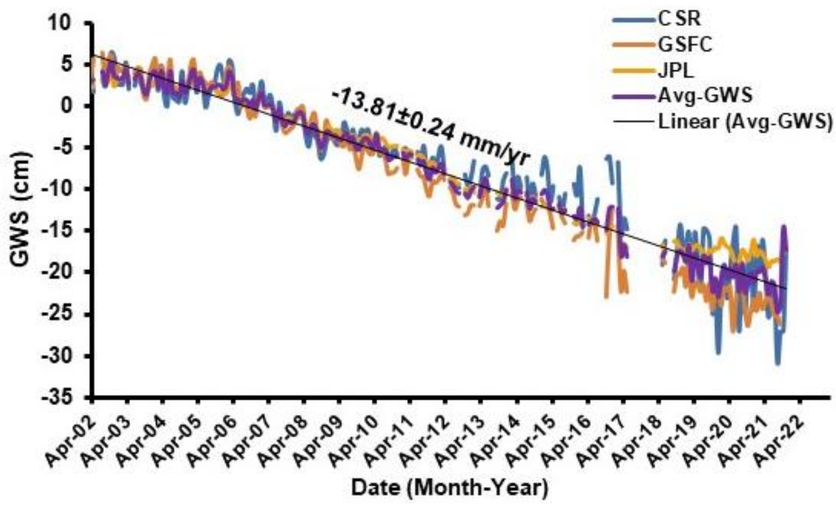

Figure 7. Monthly series and secular ΔGWS trends for the entire study area.

4.5. Anthropogenic Activities

The US Geological Survey studied Landsat datasets that included many time periods of satellite imagery and has shown the changes in the land use/land cover caused by anthropogenic activities (Figure 8 [2,72]). The 1986 Landsat image of the arid Wadi As-Sirhan region reveals almost no evidence of agriculture. In subsequent images, an increasing number of green spots appear in the desert. Each green dot represents an agricultural field irrigated by a center-pivot system. Water is piped from a subterranean aquifer to irrigate the fruit, vegetable, and wheat crops. The underground reservoir, called Al Sag in Saudi Arabia, extends into Jordan, where it is named Al-Disi. It is a fossil transboundary aquifer containing water that was collected between 10,000 and 30,000 years ago, with minimal present-day recharging. It represents a portion of the western section of the Saq-Ram Aquifer System. Extending on the ground from the northern part of Saudi Arabia into the southern part of Jordan is the Saq-Ram Aquifer System (West). It is currently being mined in locations ranging from Saudi Arabia's Tabuk Plain to Jordan's Wadi Rum, an area known as the Tabuk-Mudawwara-Disi area in this Inventory. The agricultural sector is largely responsible for the dramatic increase in groundwater extraction in the Tabuk area, which went from around 29 mcm/yr in the year 1983 to 1050–1700 mcm/yr in the year 2004. The water table dropping showed that the overexploitation was unsustainable. The water level in the Wadi As-Sirhan basin fell by 50 m during the period of 2002–2015 [39], with an average groundwater withdrawal rate of 1.7 km^3/yr. Therefore, without regulating extraction on both sides of the Saudi/Jordanian border, the resource could be depleted before it is fully exploited. In addition, extensive groundwater extraction caused by crop irrigation and agricultural growth increases the salinity of groundwater and irrigated soils. Increases in salinity are detrimental to soil structure, aggregate stability, and infiltration. Consequently, additional water and fertilizer must be introduced to the system, resulting in an increase in production costs and pressure on the system. The root development is restricted by clay particles with low permeability that swell and spread in response to the salt content of irrigation water. Therefore, less water can permeate the entire soil profile, resulting in waterlogging and perhaps increasing erosion. This puts additional pressure on the system, which in turn threatens the sustainability of linked livelihoods as well as the durability and productivity of crop production in this region. In addition, future climate change forecasts based on temperature and precipitation observations may lead to a reduction in soil recharge and infiltration.

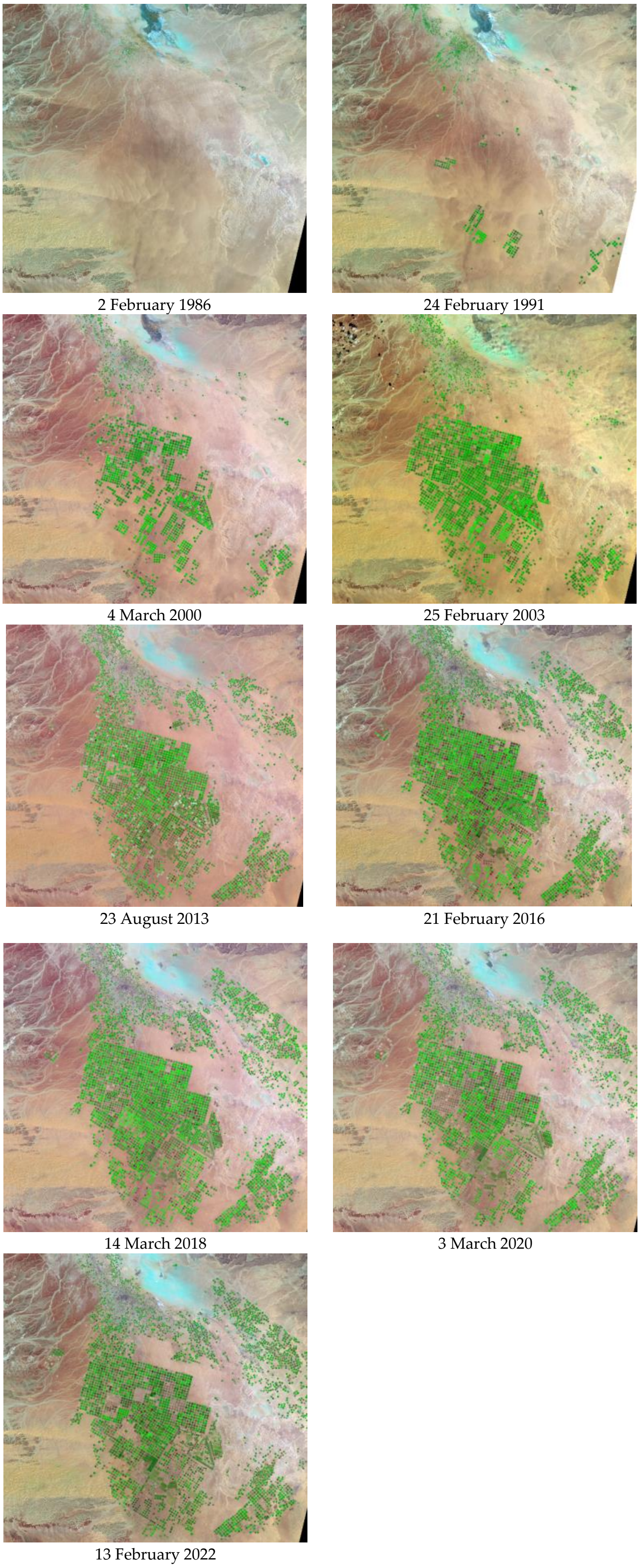

Figure 8. Images depicting the area's land use and land cover from 1986 to 2022 [72].

It may pose a concern to human health and has a possible long-term negative influence on groundwater quality.

4.6. Recharge Rate

The main factors influencing the fluctuations in ΔGWS throughout the study period are agricultural development and heavy groundwater over-exploitation. For the Wadi As-Sirhan Basin, the groundwater withdrawal varied between 1.4 and 2 km/yr during the study period of 2002–2015 [39]. By applying the maximum groundwater withdrawal rate of 2 km^3/yr for the entire period (2.0 km^3/yr; −16.12 mm/yr). The minimal recharge rate has been estimated using the following Equation (2).

$$R_n = \Delta GWS + (Q_n + Q_a) \tag{2}$$

where R_n is the natural recharge, Q_n is the natural discharge, and Q_a is the artificial discharge.

The R_n rate (Table 1) was estimated during the study period to be +2.31 ± 0.24 mm/yr by the addition of the average artificial discharge rate (−16.12 ± 0.0 mm/yr) to its ΔGWS trend (−13.81 ± 0.24 mm/yr). As a result of the lowering water table, Q_n is extremely small and negligible.

Our estimated recharge value of the Wadi As-Sirhan Basin is slightly similar to that reported by [66], where they expected that 5% or 30 mcm of the total annual precipitation of 600 mcm/yr could feed the shallow aquifer systems and be considered as a natural recharge. Calculating the average modern recharge rate, reflecting that the groundwater resources of the wadi have limited renewability, which is consistent with that estimated for the annual recharge rate of +2.31 ± 0.24 mm/yr during the study period using the GRACE datasets. This is also confirmed by the Carbon-14 and Tritium measurements, indicating that Wadi As-Sirhan's shallow deposits are receiving a modern recharge [66]. The Wadi As-Sirhan Basin's groundwater is an integral part of the groundwater system that originated in the Sakaka and Azraq regions. The groundwater of the Wadi As-Sirhan Basin and the Tabuk area to the southwest exhibit a strikingly similar isotopic signature, providing further evidence for the groundwater's origin in the southern part of the continent [66].

4.7. Sediment Thickness

Sediment thickness data were made available for download from the NOAA National Geophysical Data Center [73]. Figure 9 illustrates that the sediment thickness in the southern half of the research area increases from about 0.0 m at the southern Pre-Cambrian and Quaternary Tertiary volcanic outcrops to about 3000 m at its northern downstream, close to the Jordanian/Saudi border. This higher sediment thickness across the northern part of the country might indicate the higher groundwater reserves in the Wadi. The graben complex with a higher vertical displacement of up to 1500 m accounts for the larger sediment thickness in the wadi's central region [39,66], delimited by significant faults from the east and west. The Wadi As-Sirhan Basin is made up of depressions that are filled with sediments that range in age from the Devonian to the Neogene, including Quaternary basalt, alluvial sediments, gravels, and silt and clay that have been evaporite mineral-cemented [63].

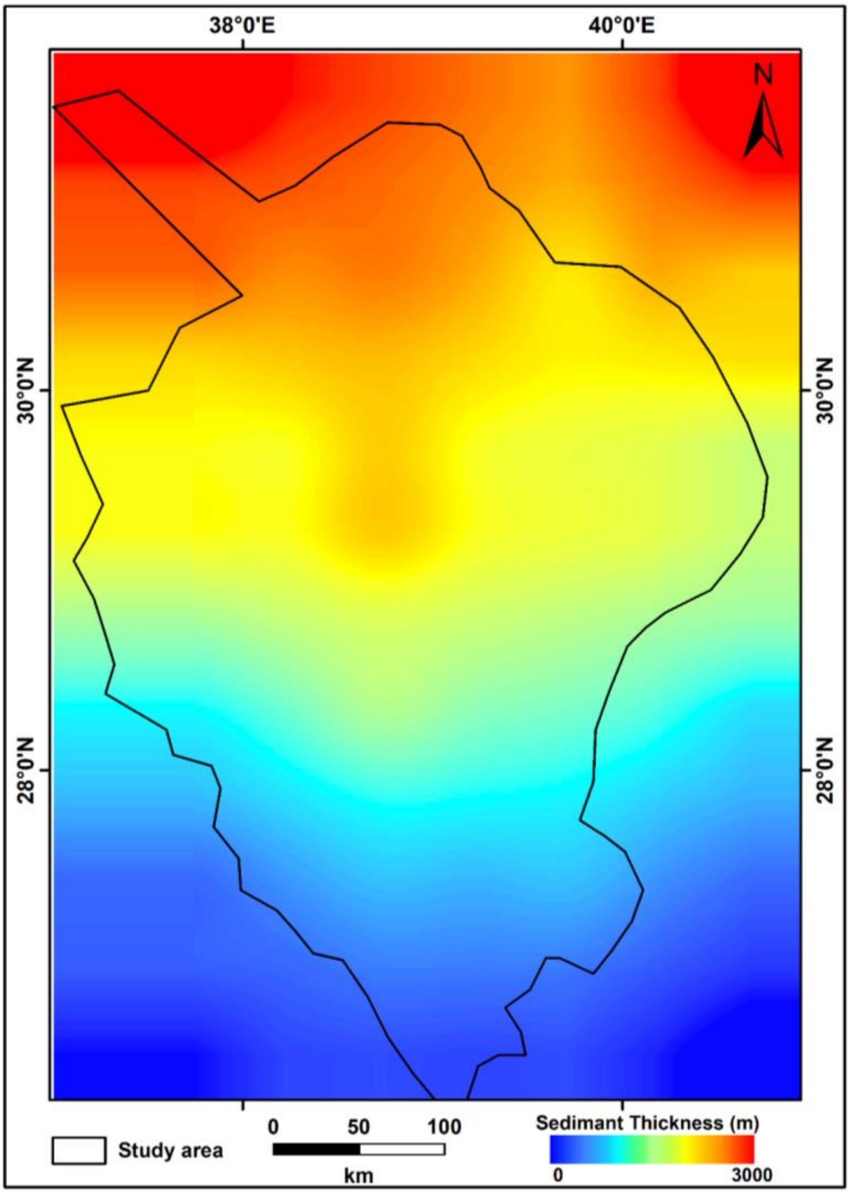

Figure 9. Thickness of the sedimentary cover (m).

4.8. Stream Networks

Figure 10 displays an ETOPO1 Global Relief Model-generated map of the study area's topography. Significant relief, from 850 to 1500 m, may be found in the southern and southeastern parts. Near to the Jordanian border in the north, the region's relief moderates to less than 500 m. Streams originate at the eastern, southern, and western parts of the wadi, and they ultimately drain into the northwestern part at its downstream. Assuming a very low precipitation rate in the south and west (Figure 3b), low surface runoff rates result in streams with low density. Consequently, the rate of recharge is minimal. Surface and groundwater flow in the southwest direction from the eastern basalt plateau and in the northeast direction from the limestone plateau. Once collected, the groundwater follows the northwest-trending main wadi stream across the Saudi/Jordanian border [66]. As may be seen in Figure 10, the Wadi As-Sirhan region has a stream order of fifth. The highest stream frequencies can be seen in first-order streams, and they gradually decrease with increasing stream orders [74]. The surface water might be carried away to the north; however, it may partially infiltrate into the underground aquifer through the permeable sand and gravel of the surface layer.

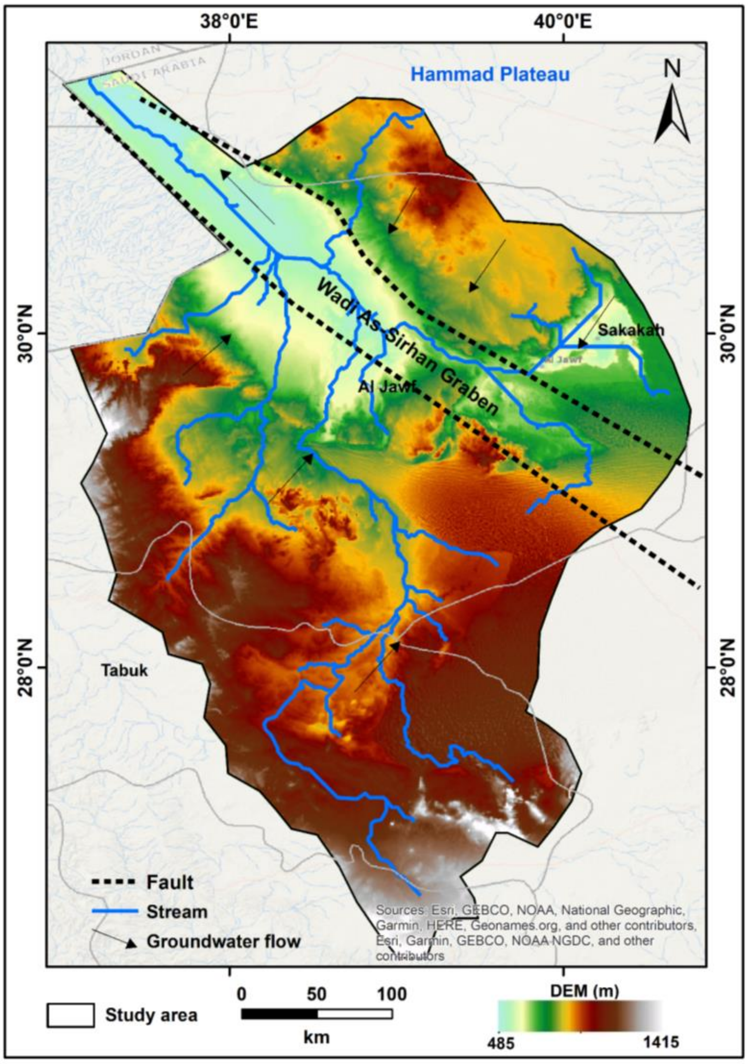

Figure 10. The DEM's elevation map of the ground's surface. Additionally depicted are the region's tributary systems.

4.9. Comparison with Conventional Approaches

Insufficient groundwater data can hamper resource management [75–78]. This is particularly true when longer time periods are necessary to evaluate an aquifer's sustainability [79]. Installing a network of monitoring wells and routinely recording, storing, and evaluating water levels and quality data over long periods is time-consuming and resource-intensive [79]. Common causes of inadequate aquifer management are due to the paucity of data and a lack of understanding of the effects of groundwater decrease [9,78,80,81]. In addition, data collection is hindered in many places of the world by a lack of ground stations, gaps in time, and restricted data interchange due to societal and political constraints [82]. Conventional approaches such as physical and chemical methods as well as modeling techniques are difficult to implement on a regional scale, and their findings are sometimes questionable due to the lack of datasets needed for their application and the substantial effort and resources necessary to collect them [36]. Utilizing recent satellite data for remote sensing monitoring could be a solution to these limitations. In addition, it frequently provides free datasets that can be used to carefully monitor hydrological variations in inaccessible locations, and for other geothermal studies and crustal structures [83,84], as well as for mineral investigations [85] and subsurface geology [86] with integrated airborne geophysical data.

5. Conclusions

Based on the satellite rainfall datasets, the Wadi As-Sirhan region is receiving a low annual precipitation rate estimated at 60 mm/yr. Therefore, the surface water resources are limited. GRACE and outputs of the GLDAS model have shown that the water resources of the wadi were subjected to groundwater depletion during the period of 2002–2021, due to the heavy groundwater withdrawal activities (−16.12 mm/yr) and agricultural development during the last 20 years. Large commercial farms using center-pivot irrigation systems have been rapidly expanding, as shown in Landsat images, and this has led to a severe overdraft of fresh groundwater from the Saudi (upstream) part of the system. For Wadi As-Sirhan, GRACE estimates the ΔGWS to be decreasing at a rate of -13.81 ± 0.24 mm/yr. The NW-trending faults that bound the Wadi As-Sirhan graben influence the groundwater and help groundwater flow in a northwesterly direction. The minor recent recharge rate, estimated at $+2.31 \pm 0.24$ mm/y for the wadi, could not compensate for the heavy groundwater withdrawal. Groundwater extraction for agricultural purposes needs to be strictly governed. Under a bilateral agreement, it is also necessary to track the rate of abstraction as well as the level and quality of the groundwater in both countries.

Author Contributions: Conceptualization, A.M. and F.A.; methodology, A.M. and F.A.; software, A.M.; validation, A.M. and F.A.; formal analysis, A.M. and F.A.; investigation, A.M. and F.A.; resources, A.M. and F.A.; data curation, A.M. and F.A.; writing—original draft preparation, A.M.; writing—review and editing, A.M.; visualization, A.M. and F.A.; supervision, A.M. and F.A.; project administration, A.M. and F.A.; funding acquisition, F.A. All authors have read and agreed to the published version of the manuscript.

Funding: This research was funded by Abdullah Alrushaid Chair for Earth Science Remote Sensing Research at King Saud University, Riyadh, Saudi Arabia.

Data Availability Statement: The data is available upon request from the authors.

Acknowledgments: The authors extend their appreciation to Abdullah Alrushaid Chair for Earth Science Remote Sensing Research for the funding.

Conflicts of Interest: The authors declare no conflict of interest.

References

1. NASA. Agricultural Fields, Wadi As-Sirhan Basin, Saudi Arabia: NASA Earth Observatory. 2012. Available online: http://earthobservatory.nasa.gov/IOTD/view.php?id=77300 (accessed on 19 December 2022).
2. Wadi As-Sirhan Basin, Saudi Arabia | EROS. Available online: Eros.usgs.gov/media-gallery/earthshot/wadi-as-sirhan-basin-saudi-arabia (accessed on 1 December 2022).
3. Watkins, M.M.; Wiese, D.N.; Yuan, D.-N.; Boening, C.; Landerer, F.W. Improved methods for observing Earth's time variable mass distribution with GRACE using spherical cap mascons. *J. Geophys. Res. Solid Earth* **2015**, *120*, 2648–2671. [CrossRef]
4. Rodell, M.; Houser, P.R.; Jambor, U.; Gottschalck, J.; Mitchell, K.; Meng, C.-J.; Arsenault, K.; Cosgrove, B.; Radakovich, J.; Bosilovich, M.; et al. The global land data assimilation system. *Bull. Am. Meteorol. Soc.* **2004**, *85*, 381–394. [CrossRef]
5. Syed, T.H.; Famiglietti, J.S.; Chen, J.; Rodell, M.; Seneviratne, S.I.; Viterbo, P.; Wilson, C.R. Tota basin discharge for the Amazon and Mississippi River basins from GRACE and a land-atmosphere water balance. *Geophys. Res. Lett.* **2005**, *32*, L24404. [CrossRef]
6. Crowley, J.W.; Mitrovica, J.X.; Bailey, R.C.; Tamisiea, M.E.; Davis, J.L. Land water storage within the Congo Basin inferred from GRACE satellite gravity data. *Geophys. Res. Lett.* **2006**, *33*, L19402. [CrossRef]
7. Crowley, J.W.; Mitrovica, J.X.; Bailey, R.C.; Tamisiea, M.E.; Davis, J.L. Annual variations in water storageand precipitation in the Amazon Basin: Bounding sink terms in the terrestrial hydrological balance using GRACE satellite gravity data. *J. Geod.* **2008**, *82*, 9–13. [CrossRef]
8. Yirdaw, S.Z.; Snelgrove, K.R.; Agboma, C.O. GRACE satellite observations of terrestrial moisture changes for drought characterization in the Canadian Prairie. *J. Hydrol.* **2008**, *56*, 84–92. [CrossRef]
9. Rodell, M.; Chen, J.; Kato, H.; Famiglietti, J.S.; Nigro, J.; Wilson, C.R. Estimating groundwater storage changes in the Mississippi River basin (USA) using GRACE. *Hydrogeol. J.* **2009**, *15*, 159–166. [CrossRef]
10. Bonsor, H.C.; Mansour, M.M.; MacDonald, A.M.; Hughes, A.G.; Hipkin, R.G.; Bedada, T. Interpretation of GRACE data of the Nile Basin using a groundwater recharge model. *Hydrol. Earth Syst. Sci.* **2010**, *7*, 4501–4533. [CrossRef]
11. Xavier, L.; Becker, M.; Cazenave, A.; Longuevergne, L.; Llovel, W.; Filho, O.C.R. Interannual variability in water storage over 2003–2008 in the Amazon Basin from GRACE space gravimetry, in situ river level and precipitation data. *Remote Sens. Environ.* **2010**, *114*, 1629–1637. [CrossRef]

12. Ahmed, M.; Sultan, M.; Wahr, J.; Yan, E.; Milewski, A.; Sauck, W.; Becker, R.; Welton, B. Integration of GRACE (Gravity Recovery and Climate Experiment) data with traditional data sets for a better understanding of the time-dependent water partitioning in African watersheds. *Geology* **2011**, *39*, 479–482. [CrossRef]
13. Wang, X.; de Linage, C.; Famiglietti, J.; Zender, C. Gravity Recovery and Climate Experiment (GRACE) detection of water storage changes in the Three Gorges Reservoir of China and comparison within situ measurements. *Water Resour. Res.* **2011**, *47*, W12502. [CrossRef]
14. Ferreira, V.G.; Gong, Z.; Andam-Akorful, S.A. Monitoring mass changes in the Volta River basin using GRACE satellite gravity and TRMM precipitation. *Bol. Ciências Geodésicas* **2012**, *18*, 549–563. [CrossRef]
15. Voss, K.A.; Famiglietti, J.S.; Lo, M.; De Linage, C.; Rodell, M.; Swenson, S. Groundwater depletion in the Middle East from GRACE with implications for transboundary water management in the Tigris–Euphrates–western Iran region. *Water Resour. Res.* **2013**, *49*, 904–914. [CrossRef] [PubMed]
16. Feng, W.; Zhong, M.; Lemoine, J.M.; Biancale, R.; Hsu, H.T.; Xia, J. Evaluation of groundwater depletion in North China using the Gravity Recovery and Climate Experiment (GRACE) data and ground-based measurements. *Water Resour. Res.* **2013**, *49*, 2110–2118. [CrossRef]
17. Gonçalvès, J.; Petersen, J.; Deschamps, P.; Hamelin, B.; Baba-Sy, O. Quantifying the modern recharge of the "fossil" Sahara aquifers. *Geophys. Res. Lett.* **2013**, *40*, 2673–2678. [CrossRef]
18. Ahmed, M.; Sultan, M.; Wahr, J.; Yan, E. The use of GRACE data to monitor natural and anthropogenic induced variations in water availability across Africa. *Earth-Sci. Rev.* **2014**, *136*, 289–300. [CrossRef]
19. Wouters, B.; Bonin, J.A.; Chambers, D.P.; Riva, R.E.M.; Sasgen, I.; Wahr, J. GRACE, Time-Varying Gravity, Earth System Dynamics and Climate Change. *Rep. Prog. Phys.* **2014**, *77*, 116801. [CrossRef]
20. Thomas, A.C.; Reager, J.T.; Famiglietti, J.S.; Rodell, M. A GRACE-based water storage deficit approach for hydrological drought characterization. *Geophys. Res. Lett.* **2014**, *41*, 1537–1545. [CrossRef]
21. Tapley, B.D.; Bettadpur, S.; Ries, J.C.; Thompson, P.F.; Watkins, M.M. GRACE measurements of mass variability in the Earth system. *Science* **2004**, *305*, 503–505. [CrossRef]
22. Cao, Y.; Nan, Z.; Cheng, G. GRACE gravity satellite observations of terrestrial water storage changes for drought characterization in the arid land of Northwestern China. *Remote Sens.* **2015**, *7*, 1021–1047. [CrossRef]
23. Huang, Z.; Pan, Y.; Gong, H.; Yeh, P.J.-F.; Li, X.; Zhou, D.; Zhao, W. Subregional-scale groundwater depletion detected by GRACE for both shallow and deep aquifers in North China Plain. *Geophys. Res. Lett.* **2015**, *42*, 1791–1799. [CrossRef]
24. Papa, F.; Frappart, F.; Malbeteau, Y.; Shamsudduha, M.; Vuruputur, V.; Sekhar, M.; Ramillien, G.; Prigent, C.; Aires, F.; Pandey, R.K.; et al. Satellite-derived surface and sub-surface water storage in the Ganges–Brahmaputra River Basin. *J. Hydrol. Reg. Stud.* **2015**, *4*, 15–35. [CrossRef]
25. Li, B.; Rodell, M. Evaluation of a model-based groundwater drought indicator in the conterminous US. *J. Hydrol.* **2015**, *526*, 78–88. [CrossRef]
26. Chinnasamy, P.; Maheshwari, B.; Prathapar, S. Understanding groundwater storage changes and rechargein Rajasthan, India through remote sensing. *Water* **2015**, *7*, 5547–5565. [CrossRef]
27. Ahmed, M.; Sultan, M.; Yan, E.; Wahr, J. Assessing and improving land surface model outputs over Africa using GRACE, field, and remote sensing data. *Surv. Geophys.* **2016**, *37*, 529–556. [CrossRef]
28. Chinnasamy, P.; Sunde, M.G. Improving spatiotemporal groundwater estimates after natural disasters using remotely sensed data-a case study of the Indian Ocean Tsunami. *Earth Sci. Inform.* **2016**, *9*, 101–111. [CrossRef]
29. Long, D.; Chen, X.; Scanlon, B.R.; Wada, Y.; Hong, Y.; Singh, V.P.; Chen, Y.; Wang, C.; Han, Z.; Yang, W. Have GRACE satellites overestimated groundwater depletion in the Northwest India Aquifer? *Sci. Rep.* **2016**, *6*, 24398. [CrossRef]
30. Lakshmi, V. Beyond GRACE: Using satellite data for groundwater investigations. *Groundwater* **2016**, *54*, 615–618. [CrossRef]
31. Castellazzi, P.; Martel, R.; Galloway, L.D.; Longuevergne, L.; Rivera, A. Assessing groundwater depletion and dynamics using GRACE and InSAR: Potential and limitations. *Groundwater* **2016**, *54*, 768–780. [CrossRef]
32. Veit, E.; Conrad, C.P. The impact of groundwater depletion on spatial variations in sea level change during the past century. *Geophys. Res. Lett.* **2016**, *43*, 3351–3359. [CrossRef]
33. Wada, Y. Modeling Groundwater Depletion at Regional and Global Scales: Present State and Future Prospects. *Surv. Geophys.* **2016**, *37*, 419–451. [CrossRef]
34. Yosri, A.M.; Abd-Elmegeed, M.A.; Hassan, A.E. Assessing groundwater storage changes in the Nubian aquifer using GRACE data. *Arab. J. Geosci.* **2016**, *9*, 567. [CrossRef]
35. Miro, M.E.; Famiglietti, J.S. Downscaling GRACE Remote Sensing Datasets to High-Resolution Groundwater Storage Change Maps of California's Central Valley. *Remote Sens.* **2018**, *10*, 143. [CrossRef]
36. Mohamed, A.; Sultan, M.; Ahmed, M.; Yan, E.; Ahmed, E. Aquifer recharge, depletion, and connectivity: Inferences from GRACE, land surface models, and geochemical and geophysical data. *Bull. Geol. Soc. Am.* **2017**, *129*, 534–546. [CrossRef]
37. Forootan, F.; Safari, A.; Mostafaie, A.; Schumacher, M.; Delavar, M.; Awange, J.L. Large-scale total water storage and water flux changes over the arid and semiarid parts of the middle east from GRACE and reanalysis products. *Surv. Geophys.* **2017**, *38*, 591–615. [CrossRef]
38. Zhao, M.; Velicogna, I.; Kimball, J.S. Satellite observations of regional drought severity in the continental United states using GRACE-based terrestrial water storage changes. *J. Clim.* **2017**, *30*, 6297–6308. [CrossRef]

39. Othman, A.; Sultan, M.; Becker, R.; Alsefry, S.; Alharbi, T.; Gebremichael, E.; Alharbi, H.; Abdelmohsen, K. Use of geophysical and remote sensing data for assessment of aquifer depletion and related land deformation. *Surv. Geophys.* **2018**, *39*, 543–566. [CrossRef]
40. Zhang, Z.; Chao, B.F.; Chen, J.; Wilson, C.R. Terrestrial water storage anomalies of Yangtze River Basin droughts observed by GRACE and connections with ENSO. *Glob. Planet. Chang.* **2015**, *126*, 35–45. [CrossRef]
41. Sun, Z.; Zhu, X.; Pan, Y.; Zhang, J.; Liu, X. Drought evaluation using the GRACE terrestrial water storage deficit over the Yangtze River Basin. *China Sci. Total Environ.* **2018**, *634*, 727–738. [CrossRef]
42. Fallatah, O.A.; Ahmed, M.; Cardace, D.; Boving, T.; Kanda, A.S. Assessment of Modern Recharge to Arid Region Aquifers Using an Integrated Geophysical, Geochemical, and Remote Sensing Approach. *J. Hydrol.* **2019**, *569*, 600–611. [CrossRef]
43. Mohamed, A. Hydro-geophysical study of the groundwater storage variations over the Libyan area and its connection to the Dakhla basin in Egypt. *J. Afr. Earth Sci.* **2019**, *157*, 103508. [CrossRef]
44. Mohamed, A. Gravity based estimates of modern recharge of the Sudanese area. *J. Afr. Earth Sci.* **2020**, *163*, 103740. [CrossRef]
45. Mohamed, A. Gravity applications in estimating the mass variations in the Middle East: A case study from Iran. *Arab. J Geosci.* **2020**, *13*, 364. [CrossRef]
46. Mohamed, A. Gravity applications to groundwater storage variations of the Nile Delta Aquifer. *J. Appl. Geophys.* **2020**, *182*, 104177. [CrossRef]
47. Abdelmohsen, K.; Sultan, M.; Save, H.; Abotalib, A.Z.; Yan, E. What can the GRACE seasonal cycle tell us about lake-aquifer interactions? *Earth-Sci. Rev.* **2020**, *211*, 103392. [CrossRef]
48. Mohamed, A.; Gonçalvès, J. Hydro-geophysical monitoring of the North Western Sahara Aquifer System's groundwater resources using gravity data. *J. Afr. Earth Sci.* **2021**, *178*, 104188. [CrossRef]
49. Taha, A.I.; Al Deep, M.; Mohamed, A. Investigation of groundwater occurrence using gravity and electrical resistivity methods: A case study from Wadi Sar, Hijaz Mountains, Saudi Arabia. *Arab. J. Geosci.* **2021**, *14*, 334. [CrossRef]
50. Mohamed, A. Constraints on the amount and passages of groundwater Flow in the Nubian Sandstone Aquifer across political boundaries, Egypt. Ph.D. Thesis, Assiut University, Asyut, Egypt, 2016; 197p.
51. Mohamed, A.; Ragaa Eldeen, E.; Abdelmalik, K. Gravity based assessment of spatio-temporal mass variations of the groundwater resources in the Eastern Desert, Egypt. *Arab. J. Geosci.* **2021**, *14*, 500. [CrossRef]
52. Mohamed, A.; Abdelrahman, K.; Abdelrady, A. Application of Time- Variable Gravity to Groundwater Storage Fluctuations in Saudi Arabia. *Front. Earth Sci.* **2022**, *10*, 873352. [CrossRef]
53. Mohamed, A.; Al Deep, M.; Othman, A.; Taha, A.I.; Alshehri, F.; Abdelrady, A. Integrated geophysical assessment of groundwater potential in southwestern Saudi Arabia. *Front. Earth Sci.* **2022**, *10*, 937402. [CrossRef]
54. Mohamed, A.; Faye, C.; Othman, A.; Abdelrady, A. Hydro-geophysical Evaluation of the Regional Variability of Senegal's Terrestrial Water Storage Using Time-Variable Gravity Data. *Remote Sens.* **2022**, *14*, 4059. [CrossRef]
55. Mohamed, A.; Abdelrady, A.; Alarifi, S.S.; Othman, A. Hydro-geophysical and Remote Sensing assessment of Chad's groundwater resources. *Remote Sens.* **2023**. *under review*.
56. Al Deep, M.; Araffa, S.A.S.; Mansour, S.A.; Taha, A.I.; Mohamed, A.; Othman, A. Geophysics and remote sensing applications for groundwater exploration in fractured basement: A case study from Abha area, Saudi Arabia. *J. Afr. Earth Sci.* **2021**, *184*, 104368. [CrossRef]
57. Fallatah, O.A.; Ahmed, M.; Save, H.; Akanda, A.S. Quantifying Temporal Variations in Water Resources of a Vulnerable Middle Eastern Transboundary Aquifer System. *Hydrol. Process.* **2017**, *31*, 4081–4091. [CrossRef]
58. Simmers, I. *Recharge of Phreatic Aquifers in (Semi-) Arid Areas: International Association of Hydrogeologists (IAH) International Contributions to Hydrogeology 19*; CRC Press: Boca Raton, FL, USA, 1997; 240p.
59. de Vries, J.J.; Simmers, I. Groundwater recharge: An overview of process and challenges. *Hydrogeol. J.* **2002**, *10*, 5–17. [CrossRef]
60. Scanlon, B.R.; Healy, R.W.; Cook, P.G. Choosing appropriate techniques for quantifying groundwater recharge. *Hydrogeol. J.* **2002**, *10*, 18–39. [CrossRef]
61. Milewski, A.; Sultan, M.; Yan, E.; Becker, R.; Abdeldayem, A.; Soliman, F.; Gelil, K.A. A remote sensing solution for estimating runoff and recharge in arid environments. *J. Hydrol.* **2009**, *373*, 1–14. [CrossRef]
62. Mohamed, A.; Ahmed, E.; Alshehri, F.; Abdelrady, A. The groundwater flow behavior and the recharge in the Nubian Sandstone Aquifer System during the wet and arid periods. *Sustainability* **2022**, *14*, 6823. [CrossRef]
63. Wallace, C.A.; Dini, S.M.; Al-Farasani, A.A. Geologic Map of Wadi As Sirhan Quadrangle, Sheet 30C, Kingdom of Saudi Arabia with Explanatory Notes: Saudi Geological Survey Geologic Map, 2000, GM-127C, 27.16 figs., 1 pl.Bottom of Form. Available online: https://pubs.er.usgs.gov/publication/i200A (accessed on 19 December 2022).
64. Powers, R.W.; Ramirez, L.F.; Redmond, C.D.; Elberg, E.L., Jr. *Geology of the Arabian Peninsula; Sedimentary Geology of Saudi Arabia: U. S. Geological Survey Professional*; Paper 560-D; United States Government Printing Office: Washington, DC, USA, 1966; p. 147. Available online: https://pubs.usgs.gov/pp/0560d/report.pdf (accessed on 19 December 2022).
65. Wagner, W. The Arabian plate: Geology and hydrogeologic characteristics. In *Groundwater in the Arab Middle East*; Springer: Dordrecht, The Netherlands, 2011; pp. 1–61.
66. UN-ESCWA; BGR. *Bundesanstalt für Geowissenschaften und Rohstoffe. Inventory of Shared Water Resources in Western Asia*; United Nations Economic and Social Commission for Western Asia: Beirut, Lebanon, 2013.

67. Luthcke, S.B.; Sabaka, T.J.; Loomis, B.D.; Arendt, A.A.; McCarthy, J.J.; Camp, J. Antarctica, Greenland, and Gulf of Alaska land-ice evolution from an iterated GRACE global mascon solution. *J. Glaciol.* **2013**, *59*, 216. [CrossRef]
68. Wiese, D.N.; Landerer, F.W.; Watkins, M.M. Quantifying and reducing leakage errors in the JPL RL05M GRACE mascon solution. *Water Resour. Res.* **2016**, *52*, 7490–7502. [CrossRef]
69. Save, H.; Bettadpur, S.; Tapley, B.D. High-resolution CSR GRACERL05 Mascons. *J. Geophys. Res. Solid Earth* **2016**, *121*, 7547–7569. [CrossRef]
70. Save, H. CSR GRACE and GRACE-FO RL06 Mascon Solutions v02. *Mascon Solut.* **2020**, *12*, 24.
71. Hogue, T.S.; Bastidas, L.; Gupta, H.; Sorooshian, S.; Mitchell, K.; Emmerich, W. Evaluation and Transferability of the Noah Land Surface Model in Semiarid Environments. *J. Hydrometeorol.* **2005**, *6*, 68–84. Available online: https://journals.ametsoc.org/view/journals/hydr/6/1/jhm-402_1.xml (accessed on 20 August 2022). [CrossRef]
72. Available online: https://eros.usgs.gov/media-gallery/earthshot/wadi-as-sirhan-basin-saudi-arabia (accessed on 1 December 2022).
73. Divins, D. *Total Sediment Thickness of the World's Oceans and Marginal Seas*; NOAA National Geophysical Data Center: Boulder, CO, USA, 2003.
74. Pareta, K.; Pareta, U. Quantitative Morphometric Analysis of a Watershed of Yamuna Basin, India Using ASTER (DEM) Data and GIS. *Int. J. Geomat. Geosci.* **2011**, *2*, 248–269.
75. Purdy, A.J.; David, C.H.; Sikder, M.; Reager, J.T.; Chandanpurkar, H.A.; Jones, N.L.; Matin, M.A. An Open-Source Tool to Facilitate the Processing of GRACE Observations and GLDAS Outputs: An Evaluation in Bangladesh. *Front. Environ. Sci.* **2019**, *7*, 155. [CrossRef]
76. Wada, Y.; Wisser, D.; Bierkens, M.F.P. Global modeling of withdrawal, allocation and consumptive use of surface water and groundwater resources. *Earth Syst. Dynam.* **2014**, *5*, 15–40. [CrossRef]
77. Famiglietti, J.S. The Global Groundwater Crisis. *Nat. Clim. Chang.* **2014**, *4*, 945–948. [CrossRef]
78. Barbosa, S.A.; Pulla, S.T.; Williams, G.P.; Jones, N.L.; Mamane, B.; Sanchez, J.L. Evaluating Groundwater Storage Change and Recharge Using GRACE Data: A Case Study of Aquifers in Niger, West Africa. *Remote Sens.* **2022**, *14*, 1532. [CrossRef]
79. McStraw, T.C.; Pulla, S.T.; Jones, N.L.; Williams, G.P.; David, C.H.; Nelson, J.E.; Ames, D.P. An Open-Source Web Application for Regional Analysis of GRACE Groundwater Data and Engaging Stakeholders in Groundwater Management. *JAWRA J. Am. Water Resour. Assoc.* **2021**, *58*, 1002–1016. [CrossRef]
80. Famiglietti, J.S.; Rodell, M. Water in the Balance. *Science* **2013**, *340*, 1300–1301. [CrossRef]
81. Villholth, K.G. Groundwater Assessment and Management: Implications and Opportunities of Globalization. *Hydrogeol. J.* **2006**, *14*, 330–339. [CrossRef]
82. Skaskevych, A.; Lee, J.; Jung, H.; Bolten, J.; David, J.; Policelli, F.; Goni, I.; Favreau, G.; San, S.; Ichoku, C. Application of GRACE to the estimation of groundwater storage change in a data-poor region: A case study of Ngadda catchment in the Lake Chad Basin. *Hydrol. Process.* **2020**, *34*, 941–955. [CrossRef]
83. Mohamed, A.; Al Deep, M.; Abdelrahman, K.; Abdelrady, A. Geometry of the magma chamber and curie point depth beneath Hawaii Island: Inferences from magnetic and gravity data. *Front. Earth Sci.* **2022**, *10*, 847984. [CrossRef]
84. Mohamed, A.; Al Deep, M. Depth to the bottom of the magnetic layer, crustal thickness, and heat flow in Africa: Inferences from gravity and magnetic data. *J. Afr. Earth Sci.* **2021**, *179*, 104204. [CrossRef]
85. Mohamed, A.; Abdelrady, M.; Alshehri, F.; Mohammed, M.A.; Abdelrady, A. Detection of Mineralization Zones Using Aeromagnetic Data. *Appl. Sci.* **2022**, *12*, 9078. [CrossRef]
86. Mohamed, A.; Abu El Ella, E.M. Magnetic applications to subsurface and groundwater investigations: A case study from Wadi El Assiuti, Egypt. *Int. J. Geosci.* **2021**, *12*, 77–101. [CrossRef]